BSuD93.pdf

Photoacoustic Microscopy and Spectroscopy of Individual Red Blood Cells

Min Rui[1], Wolfgang Bost[2], Eike C. Weiss[3], Robert Lemor[2] and Michael C. Kolios[1]

[1]Dept. of Physics, Ryerson University, 350 Victoria St., Toronto, ON, Canada,
[2]Fraunhofer Institute for Biomedical Technology, St. Ingbert, Germany
[3]kibero GmbH, Saarbrücken, Germany
mkolios@ryerson.ca

Abstract: Optoacoustic imaging relies on the ultrasonic detection of pressure waves created after optical absorption. In this work we demonstrate imaging single red blood cells using an ultrasonic detection system at 200 and 400 MHz.

OCIS codes: (170.3880) Medical and biological imaging; (350.0350) Other areas of optics

1. Introduction

There has been great interest and progress in the field of optoacoustic imaging for biomedical applications. In optoacoustic imaging pressure transients created by thermoelastic expansion after optical absorption are used to create an image that maps the optical and thermoelastic properties of tissue. The pressure transients can be detected with conventional ultrasonic technologies. It has been shown theoretically that the frequency content of the ultrasonic signals produced are related to the laser pulse width and the size of the optical absorber[1, 2]. This suggests that optoacoustic imaging can be used to perform not only spectroscopic imaging (by changing the laser wavelength) but also ultrasonic spectroscopy that is related to the size of the absorbing object (by analyzing the frequency content of the ultrasound signals detected). This approach is well known in the field of ultrasound tissue characterization in which the frequency content of the scattered ultrasound can be related to the size and spatial distribution of the scattering structures within the tissue[3-5]. In this work we demonstrate that the pressure transients produced in optoacoustic imaging can be detected in the ultrasonic range spanning 100 to 500 MHz from micron sized objects. This was done by imaging individual red blood cells in solution. Moreover, we show the frequency content of the radiofrequency signals detected by the ultrasound transducers and demonstrate the potential of optoacoustic spectroscopy based on analysis of the ultrasound frequency spectra collected.

2. Materials and methods

Sheep red blood cells (suspended at 10% in PBS) were purchased from Innovative Research (Michigan, USA). Cells were diluted in coupling medium: DMEM with 10%FBS (Invitrogen Canada Inc., Burlington, Ontario, Canada) plus 10mM of MES solution (Sigma-Aldrich), and seeded to the Lab-Tek II chambered cover glass (Nunc, Thermo Fisher Scientific, Rochester, USA). The cover glass was pre-coated with Cell-TAK adhesive reagent (BD Biosciences, Bedford, MA, USA) according to manufacturer's protocol. The chambered cover glass was transferred to the microscope at which they were maintained at 37°C during all measurements.

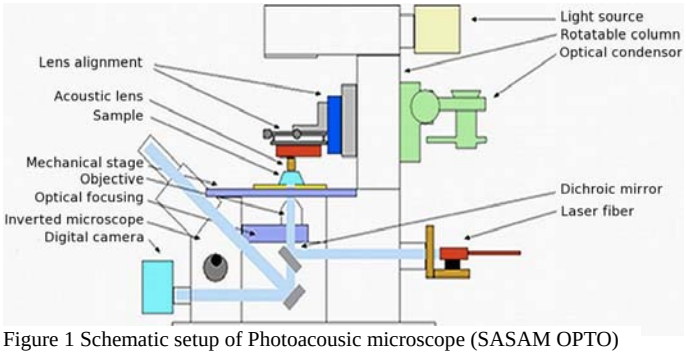

Figure 1 Schematic setup of Photoacousic microscope (SASAM OPTO)

The photoacoustic microscope combines the SAarland Scanning Acoustic Microscope (SASAM, Kibero GmbH, Saarbrücken,Germany) with an optical irradiation module (SASAM OPTO, Fraunhofer, IBMT, Germany). The SASAM OPTO module is a compact unit for generating ultra short laser pulses (700 ps) with high repetition rates. 1064nm pulses are generated from a diode pumped passively Q-switched Nd:YAG microchip engine (teemphotonics TM, Soliton Laser-und Messtechnik GmbH, Germany).

The schematic setup of photoacoustic microscope is shown in Figure 1. The acoustic microscope (SASAM) consists of an inverted optical microscope (Olympus IX81,Tokyo, Japan) with an acoustic scanning unit attached to a rotating column that allows exchanging of the transillumination condenser and the acoustic scanning unit[6]. This enables us to record optical trans-illumination and acoustic data of the same cell. In this study, two types of

acoustical lens were used operating at 205MHz and 375MHz. The acoustic lens characteristics are shown in Table 1. Besides the controlling of the laser, the SASAM OPTO features also one built in manual switch for changing between pure acoustic and optoacoustic mode, which allows the recording of acoustic, photoacoustic and optical data from the same sample (red blood cell in this work). A custom-built Labview based software, the OptoAcoustic Investigator (Fraunhofer, IBMT, Germany), was used for controlling acoustic and photoacoustic data acquisition. The acoustic lens and the laser beam are confocally aligned: firstly, the acoustic lens was aligned with the optical path under the guidance of the optical objective; then using a black permanent marker dot on the cover glass, the laser beam and the acoustic lens were precisely aligned by scanning on the piezo scanning stage until the signal was maximized. The ultrasonic signals generated by the photoacoustic excitation of the sample were detected by the piezoelectric transducer. The sample is scanned mechanically line by line in a raster pattern. The lateral (x-y) scanning was performed using the movement of sample stage with a step size of 1um. While scanning the sample, the RF-signal is being recorded and digitized. The digitization rate for the amplified RF signal was 8GSamples/s and the digitization resolution was 8 bit[6]. The phase-contrast optical images were taken by the Olympus IX81 inverted microscope after each photoacoustic imaging scan.

The software package provided by Kibero (Kibero GmbH, Saarbrücken,Germany) called Acoustic Researcher was used, which allows a quick analysis of the saved data. The signals can be filtered and gated to specific regions of the data and A-scan, B-scan and C-scan can be displayed[6]. Spectral analysis of data was performed using MATLAB (The Mathworks Inc., Natich, MA, USA). The Fourier transform was computed. The squared magnitudes of the resultant spectra were averaged and divided by the power spectrum computed from the acoustic signal reflection from a glass substrate (in pulse echo mode) to calculate the transfer function of the acoustic system and compute the normalized power spectra[7]. This procedure removed system and transducer transfer functions to provide a common reference for data collected using various transducers[3, 8]. Linear regression analysis was used to calculate the spectral slope from the normalized backscatter power.

3. Results

The results from imaging a single red blood cell are shown in Figure 2. In the panel A, a phase contrast image of a red blood cell is shown. The optoacoustic images generated from the cell at 205 and 375 MHz are shown in the two panels adjacent to the optical image. To our best knowledge, these are the first optoacoustic images produced of individual red blood cells. Striations in the image are caused by motion of the red blood cell during the scanning of the acoustic tip above the cell. Representative radiofrequency lines detected by the ultrasound transducer are shown in panel B. It can be appreciated that there is a very high signal-to-noise that is generated when irradiating the red blood cell, even at the optical wavelength of 1064 nm (far from the absorption peak of the red blood cell). In panel C the power spectra of the signal from the cells and the reflection off a glass plate (in an acoustic pulse-echo experiment) are compared. The data collected from the 205 MHz transducer illustrate the similarity of the power spectra from the signals produced from the red blood cells to the sensitivity band of the transducer over the range of 140 to 260 MHz (the -6dB bandwidth of the transducer sensitivity profile). The data collected using the 375 MHz transducer (panel C., to the right) also compares the relative power spectra of the reference and the optoacoustic signal from the red blood cells. Here it can be appreciated that the signal from the red blood cells differs from the reference signal, illustrating a frequency dependence of the signal produced by the red blood cells. The frequency dependence of the signal could be used to infer the size of the absorbing structure. Moreover, the consistency of the signals produced for 10 different red blood cells within the field of view of the optical microscope illustrates the reproducibility of the measurement (individual traces in the power spectra in panel C.). The normalized curves (panel D.) illustrate how the spectral amplitude changes with frequency for the two transducers that are used. As these are preliminary experiments, there are no corrections for ultrasonic attenuation through the medium (which is significant at these high frequencies) and the diffraction field of the ultrasonic transducer. These are common corrections that are required in the field of ultrasonic tissue characterization[9].

4. Conclusions

Here we show, for the first time, optoacoustics images of individual red blood cells. This illustrates that the signals produced by such micron size biological specimens can be detected by the appropriate ultrasound transducers and images with very high signal-to-noise can be produced. Moreover, we illustrate the principle of ultrasonic spectroscopy for the elucidation of microstructure based on the frequency dependence of the ultrasonic signals produced which depend on the size of the optical absorber. Future work will include the imaging of mammalian

cells and the rigorous correction for attenuation through the medium and the diffraction field of the ultrasound transducers.

References

1. Wang, L.V., Prospects of photoacoustic tomography. Med Phys, 2008. 35(12): p. 5758-67.
2. Diebold, G.J., M.I. Khan, and S.M. Park, Photoacoustic "Signatures" of Particulate Matter: Optical Production of Acoustic Monopole Radiation. Science, 1990. 250(4977): p. 101-104.
3. Kolios, M.C., et al., Ultrasonic spectral parameter characterization of apoptosis. Ultrasound Med Biol, 2002. 28(5): p. 589-97.
4. Oelze, M.L., et al., Differentiation and characterization of rat mammary fibroadenomas and 4T1 mouse carcinomas using quantitative ultrasound imaging. IEEE Trans Med Imaging, 2004. 23(6): p. 764-71.
5. Insana, M.F. and T.J. Hall, Characterising the microstructure of random media using ultrasound. Phys Med Biol, 1990. 35(10): p. 1373-86.
6. Weiss, E.C., et al., Mechanical properties of single cells by high-frequency time-resolved acoustic microscopy. IEEE Trans Ultrason Ferroelectr Freq Control, 2007. 54(11): p. 2257-71.
7. Lizzi, F.L., et al. Ultrasonic spectrum analysis for assays of different scatterer morphologies: theory and very-high frequency clinical results. in Proceedings of the 1996 IEEE Ultrasonics Symposium. Part 2 (of 2), Nov 3-6 1996. 1996. San Antonio, TX, USA: IEEE, Piscataway, NJ, USA.
8. Vlad, R.M., et al., Quantitative ultrasound characterization of cancer radiotherapy effects in vitro. Int J Radiat Oncol Biol Phys, 2008. 72(4): p. 1236-43.
9. Bigelow, T.A. and W.D. O'Brien, Jr., Scatterer size estimation in pulse-echo ultrasound using focused sources: calibration measurements and phantom experiments. J Acoust Soc Am, 2004. 116(1): p. 594-602.

Table 1. Characteristics of acoustic lenses.

Center Frequency (MHz)	FWHM (MHz)	Focal Length (μm)	Aperture Width (μm)	Aperture Angle	Axial Res. (μm)	Lateral Res. (μm)	Depth of Field (μm)
205	145-235	500	500	60	8.3	7.3	71.0
375	20-440	350	300	60	3.9	4.7	52.8

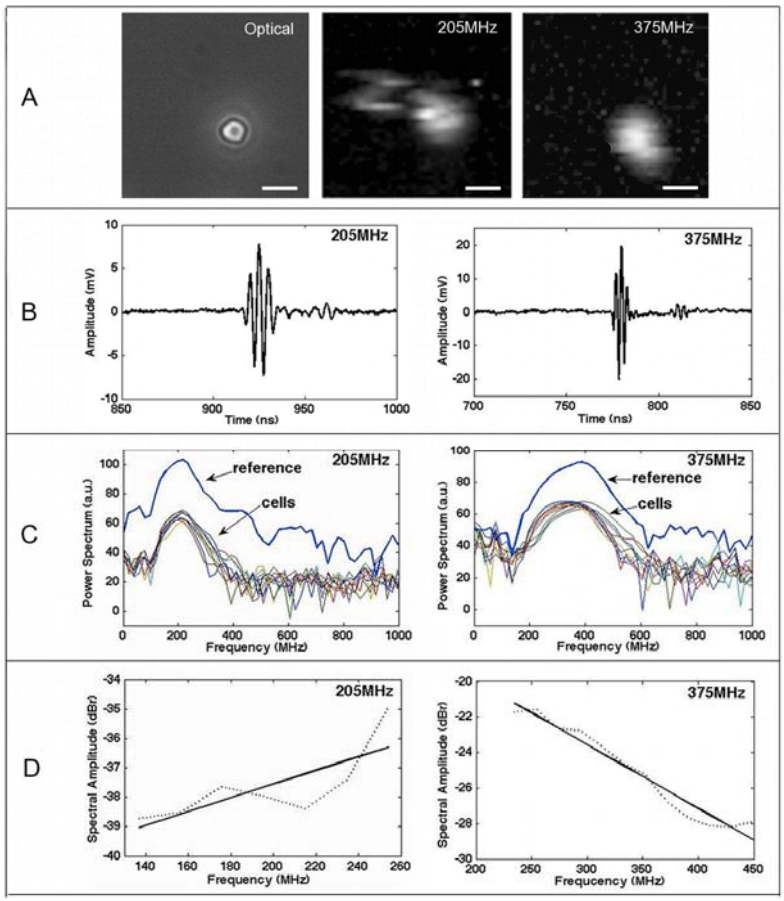

Figure 2 Red blood cell photoacoustic images and signal analysis. Panel A. Red blood cell optical image and photoacoustic C-scan images at 205MHz and 375MHz, respectively. Panel B. Representative photoacoustic signals from red blood cell at two central frequencies: 205MHz and 375MHz, respectively. Panel C. Plot of power spectrum of reference (glass acoustic signal) and individual red blood cells (10 cells for each frequency) at central frequency of 205MHz and 375MHz, respectively. Panel D. Spectral slope of red blood cell photoacoustic signal at central frequency of 205MHz and 375MHz, respectively. Scale bars show 10μm.